ELSEVIER

Biochimica et Biophysica Acta 1514 (2001) 127–138

BIOCHIMICA ET BIOPHYSICA ACTA
BBA

www.bba-direct.com

Interleukin-2-induced small unilamellar vesicle coalescence

Larry T. Boni [a], Michael M. Batenjany [a,*], Mary E. Neville [a], Yuqing Guo [a], Linda Xu [a], Fangjun Wu [a], Jeffrey T. Mason [b], Richard J. Robb [a], Mircea C. Popescu [a]

[a] *Biomira USA Inc., 1002 Eastpark Blvd., Cranbury, NJ 08512, USA*
[b] *Department of Cellular Pathology, Armed Forces Institute of Pathology, Rockville, MD 20850, USA*

Received 18 January 2001; received in revised form 15 June 2001; accepted 19 June 2001

Abstract

Recombinant human interleukin-2 (rhIL-2) was incorporated in liposomes for potential therapeutic applications using a novel process. In this process, rhIL-2 caused the formation of large, unique multilamellar vesicles (MLVs) from small unilamellar vesicles (SUVs) of dimyristoylphosphatidylcholine (DMPC). Vesicle coalescence occurred most rapidly at 19°C, between the pre- and main phase transition temperatures of DMPC, and showed a dependence upon pH (pH < 5.5), ionic strength (> 50 mM) and the initial size of the unilamellar vesicles (≤ 25 nm). Intermediates (partially coalesced vesicles) within the forming multilamellar structures were identified by freeze-fracture electron microscopy and their presence was corroborated by differential scanning calorimetry. Several distinct steps were identified in the coalescence process. In the initial step, rhIL-2 rapidly bound to the DMPC SUVs. This was followed by a pH-dependent conformational change in the protein, as evidenced by an increase in tryptophan fluorescence intensity. The SUVs then aggregated in large clusters that eventually annealed to form closed MLVs. In this process over 90% of the rhIL-2 was bound to and incorporated within the multilamellar structures.

Keywords: Interleukin-2; Liposome; Small unilamellar vesicle; Fusion; Lipid–protein interaction

1. Introduction

Human interleukin-2 (IL-2) is a 15.5 kDa monomeric protein composed primarily of a bundle of four α-helices [1,2]. Produced principally by T-lymphocytes of the Th1 helper cell subtype [3], IL-2 plays a role in the amplification of both humoral and cell-mediated immunity [4–7]. It promotes the proliferation of antigen-activated T-lymphocytes of the helper and cytotoxic phenotypes, facilitates tumor killing by activated macrophages, natural killer cells and lymphokine-activated killer cells and increases antibody production by B-cells. Recombinant human interleukin-2 (rhIL-2) has shown promise as a direct therapeutic agent [8–10] and is now approved for two indications, renal cell carcinoma and malignant melanoma. The systemic toxicity of rhIL-2, however, has limited its clinical application [11].

rhIL-2 has been incorporated in liposomes for use in cancer immunotherapy. The potential medical significance of such formulations is emphasized by the many preclinical studies showing that liposomal rhIL-2 is less toxic and more efficacious than free rhIL-2 [12–22]. This improved therapeutic index

* Corresponding author. Fax: 609-655-1755.
E-mail address: mbatenjany@biomira.com (M.M. Batenjany).

0005-2736/01/$ – see front matter
PII: S0005-2736(01)00377-7

may be due to a liposome-dependent alteration of the protein's biodistribution and biopharmaceutics. Incorporation of rhIL-2 into multilamellar liposomes increased the serum half-life about 4-fold and caused accumulation in the reticuloendothelial system (RES), including lymphoid organs such as the spleen and lymph nodes [23,24]. Other potentially advantageous attributes of such formulations included specific binding of the liposomes to immune cells expressing the IL-2 receptor [25] and the slow release of free rhIL-2 under physiological conditions [25]. Incorporation of rhIL-2 into liposomes composed of dimyristoylphosphatidylcholine (DMPC) has been accomplished using standard methods such as hydration from a thin film or multiple freeze–thaw cycles [19,23]. The fact that the incorporation was relatively high (greater than 50%) implied the existence of a direct interaction between rhIL-2 and lipid. This would be consistent with studies showing that proteins and peptides which possess amphipathic helices, like IL-2, interact with lipid bilayers [26–29].

In studying the interaction between rhIL-2 and DMPC, we noticed that rhIL-2 had the ability to cause small unilamellar vesicles (SUVs) of DMPC to form large, unique, multilamellar vesicles (MLVs) with a mean diameter typically greater than 2 μm. Freeze-fracture electron microscopy and vesicle leakage experiments defined this process to be coalescence and not fusion. The vesicles first aggregated in large clusters of leaky SUVs that annealed in time to form closed multilamellar bilayers. In this manuscript, the kinetics and characteristics of this MLV formation and its dependence on such factors as temperature, pH, ionic strength and SUV size are examined. This process, in which over 90% of the rhIL-2 was bound to and incorporated within multilamellar structures, represents a novel method of formulating liposomes for therapeutic purposes.

2. Methods

2.1. Materials

rhIL-2 was provided by Hoffmann-LaRoche (Nutley, NJ) or manufactured at Biomira (Edmonton, Alberta, Canada) using the Hoffmann-LaRoche process. The purified protein was stored in 50 mM sodium acetate, pH 3.5 containing 5 mg/ml mannitol. In some experiments rhIL-2 was dialyzed against 1 mM phosphate buffer, pH 7. Dimyristoylphosphatidycholine (DMPC), dipalmitoylphosphatidylcholine (DPPC), egg phosphatidylcholine (EPC), dimyristoylphosphatidylglycerol (DMPG), *N*-(7-nitro-2-1,3-benzoxadiazol-4-yl)dimyristoylphosphatidylethanolamine (NBD-PE), *N*-(lissamine rhodamine B sulfonyl)dimyristoylphosphatidylethanolamine (Rhod-PE) and cholesterol were manufactured by Avanti Polar Lipids (Pelham, AL). *N*-Bromosuccinimide was purchased from Sigma (St. Louis, MO). All other fluorescent probes and quenchers were obtained from Molecular Probes (Junction City, OR). Alamar blue was purchased from Biosource International (Camarillo, CA). Microcon 100 filters were from Amicon (Beverly, MA).

2.2. SUV formation

MLVs were formed by direct hydration above the main phase transition temperature of DMPC. Typically 0.8 ml of 1 mM phosphate buffer pH 7, 0.9% saline at 37°C was added to 200 mg of DMPC. For mixtures of lipids, the lipids were first dissolved in chloroform, following which a thin film was formed in a round bottom flask by evaporation of the chloroform on a rotary evaporator. The thin film was subsequently hydrated as above. SUVs of ≤ 25 nm mean diameter were formed from MLVs by size reduction employing either a bath sonicator (Model G112SPIT, Laboratory Supplies, Hicksville, NY) or a homogenizer such as a Gaulin Rannie APV Model Mini-Lab type 7.30VH (Wilmington, MA).

2.3. Large unilamellar vesicle (LUV) formation

LUVs were formed by extrusion of MLVs through two stacked Nucleopore polycarbonate filters (Pleasantville, CA) in an Extruder device (Lipex, Vancouver, BC, Canada). The MLVs were appropriately size reduced by sequential passage (5–10 passes each) through stacked filters of pore sizes 1.0, 0.4, 0.2, 0.08, 0.05, and 0.03 μm.

2.4. rhIL-2-induced coalescence process

DMPC SUVs or LUVs were incubated with rhIL-2 at a lipid:rhIL-2 mass ratio of 250:1. Temperature, incubation time, pH and ionic strength were varied as described in the text. During pH experiments, small amounts of 100 mM sodium citrate buffer were used, i.e., the overall ionic strength was increased approx. 11% (e.g. 50→56, 100→110, 150→165 mM). Optimal coalescence was observed after 24 h incubation at 19°C using limit size DMPC SUVs (≤25 nm). The SUVs were prepared in 150 mM NaCl containing 1 mM sodium phosphate buffer with the pH adjusted to pH 4 with sodium citrate, as described above.

2.5. Turbidity

Coalescence or aggregation was monitored by turbidity at 660 nm on a Shimadzu UV-160U UV-Vis spectrophotometer (Tokyo, Japan). Aliquots for time points were diluted to 2 mg/ml DMPC prior to measurement. Coalescence was confirmed by light microscopy.

2.6. Leakage assay

DMPC SUVs were formed in the presence of 10 mM 8-aminonaphthalene-1,3,6-trisulfonic acid (ANTS) and 32 mM *p*-xylylene-bis-pyridinium bromide (DPX). At these concentrations the DPX quenches the ANTS. The SUVs were washed by dialysis and incubated in the presence of rhIL-2 (DMPC/IL-2 at 250:1, mass ratio) at different temperatures. 100% leakage is determined by lysing the SUVs with *n*-octyl glucoside. Measurements were performed on a PTI QM-1 Luminescence Spectrometer (Photon Technology International, South Brunswick, NJ) with the excitation at 354 nm and the emission at 370–600 nm.

2.7. Tryptophan fluorescence

Tryptophan (in rhIL-2) fluorescence experiments were performed using a PTI QM-1 Luminescence Spectrometer by exciting at 295 nm and recording the emission between 310 and 400 nm. The temperature was controlled (±1°C) by a Model RTE-100 water bath (Neslab Instruments, Portsmouth, NH). Typically, 0.3–3.0 μg of rhIL-2 in 3.0 ml aqueous buffer was used. This sample could be completely quenched for use as a background scatterer by adding 5 μl of a freshly prepared 10 mM *N*-bromosuccinimide solution. The 'pure' rhIL-2 tryptophan spectrum was obtained by subtracting the corresponding background ('quenched' spectrum).

2.8. Lipid mixing

MLVs were prepared by the thin film method containing DMPC, NBD-PE and rhodamine-PE at a molar ratio of 98.8:0.4:0.8 [30]. These were sonicated to form SUVs. The SUVs were mixed with blank (non-fluorescent) DMPC SUVs at a 1:19 mass ratio and incubated with and without rhIL-2. Excitation was at 470 nm, with emission measured between 485 and 650 nm. The extent of energy transfer was monitored by the ratio of peak intensities of NBD/rhodamine (520 nm and 586 nm, respectively) of the sample compared to that of a standard curve. The standard curve was generated for complete mixing at different ratios of blank to fluorescent SUVs that were co-solubilized in chloroform/methanol (2:1). The solvent was first evaporated with a stream of nitrogen gas, then further dried under vacuum to a thin film. The film was subsequently hydrated to form MLVs.

2.9. % MLV formation

The % MLV formation was defined as the total lipid minus the lipid remaining in the supernatant following centrifugation at 39 000×*g* for 30 min at 4°C, as determined by phosphate analysis [31].

2.10. IL-2 content, purity and incorporation

Total rhIL-2 was determined by a biological assay employing an IL-2-dependent cell line, CTLL-2 [32], and a standard IL-2 preparation calibrated in International Units [33]. Diluted samples were added to microtiter plates followed by the addition of CTLL-2 cells. Alamar Blue™, an oxidation–reduction indicator that changes color in response to metabolites released by the CTLL-2 cells, was used to monitor cellular proliferation [34]. To determine the incorpo-

ration of rhIL-2 in the liposomes, the samples were diluted 1/100 in PBS containing 2 mg/ml HSA and fractionated by centrifugation through Microcon® 100 filters at 2700×*g* for 15 min at 4°C. The filtrate was assayed by the CTLL assay.

2.11. Particle sizing

Particle sizing for micron range liposomes was performed on an AccuSizer 770 Optical Particle Sizer (Particle Sizing Systems, Santa Barbara, CA.) This works on the principle of single particle optical sensing, where a sample is autodiluted such that one particle at a time is counted. A NICOMP submicron C370 instrument (Particle Sizing Systems) based on dynamic light scattering was used for measuring particles below 1 μm, in particular SUVs and LUVs.

2.12. Electron microscopy

Samples without cryoprotectant were placed between copper specimen carriers and rapidly plunged into liquid propane. Fracturing and replicating was performed at −115°C in a Balzers BAF 400T Freeze-Etch unit (Liechtenstein). Cleaned replicas were viewed on a Philips EM 300 transmission electron microscope at a typical magnification of 27 000 times.

2.13. Differential scanning calorimetry (DSC)

DSC runs were performed on a CSC 4100 Multicell Differential Scanning Calorimeter (Calorimetry Sciences Corp., Provo, UT). Normal saline solution was used for baseline subtraction. Baseline subtraction, correction for the thermal instrument response and conversion to heat capacity (μJ/°C) as a function of temperature were performed using software supplied by CSC. The calorimetric data were imported into Grams/32, v.5.0 (Galactic Industries Corp., Salem, NH) for baseline and offset correction, smoothing and plotting. Data were not smoothed or only minimally smoothed by using a Savitsky–Golay smoothing routine. This method uses a convolution approach and performs a least squares fit to a specified window. When data were smoothed a 3rd order polynomial and a window of 5–11 data points were typically employed. Scan rates were run at 20°C/h in both heating and cooling directions.

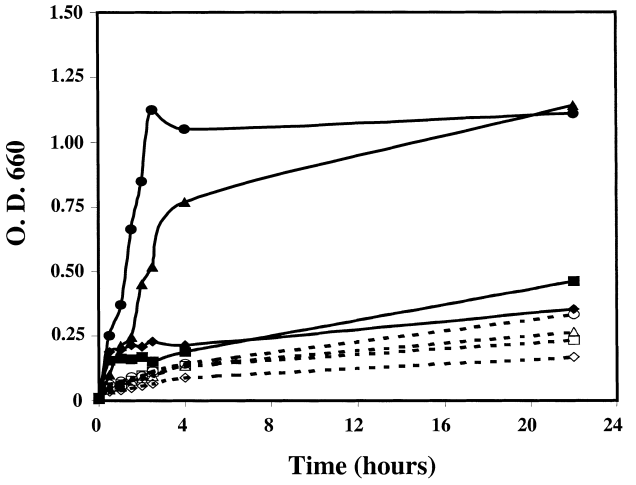

Fig. 1. The effect of temperature on the kinetics of DMPC SUV coalescence as measured by turbidity. The DMPC/rhIL-2 mass ratio is 250:1. The temperatures were 4°C (▲), 19°C (●), 23.5°C (◆), and 38°C (■). Dashed lines with corresponding unfilled symbols denote SUVs incubated in the absence of rhIL-2.

3. Results

Saturated lecithins are known to undergo both a pretransition and a main phase transition. For DMPC these occur at about 15.5°C and 24°C, respectively [35]. To determine the effect of the lipid phase on the interaction between rhIL-2 and SUVs, the rhIL2-induced formation of multilamellar vesicles was studied at various temperatures. DMPC SUVs were mixed with rhIL-2 at a lipid:protein mass ratio of 250:1 at pH 4 in 150 mM NaCl and incubated at 4, 19, 23.5 and 38°C. An increase in turbidity over time was observed at all temperatures examined (Fig. 1). The efficiency of MLV formation

Table 1
Leakage experiments[a] of DMPC SUVs (250 mg/ml) at 19°C

Time (h)	w/rhIL-2 (% leakage)	Control (% leakage)
6	~12	<2
12	~20	<2
24	~28	<2

[a]DMPC SUVs were preloaded with 10 mM ANTS and 32 mM DPX.

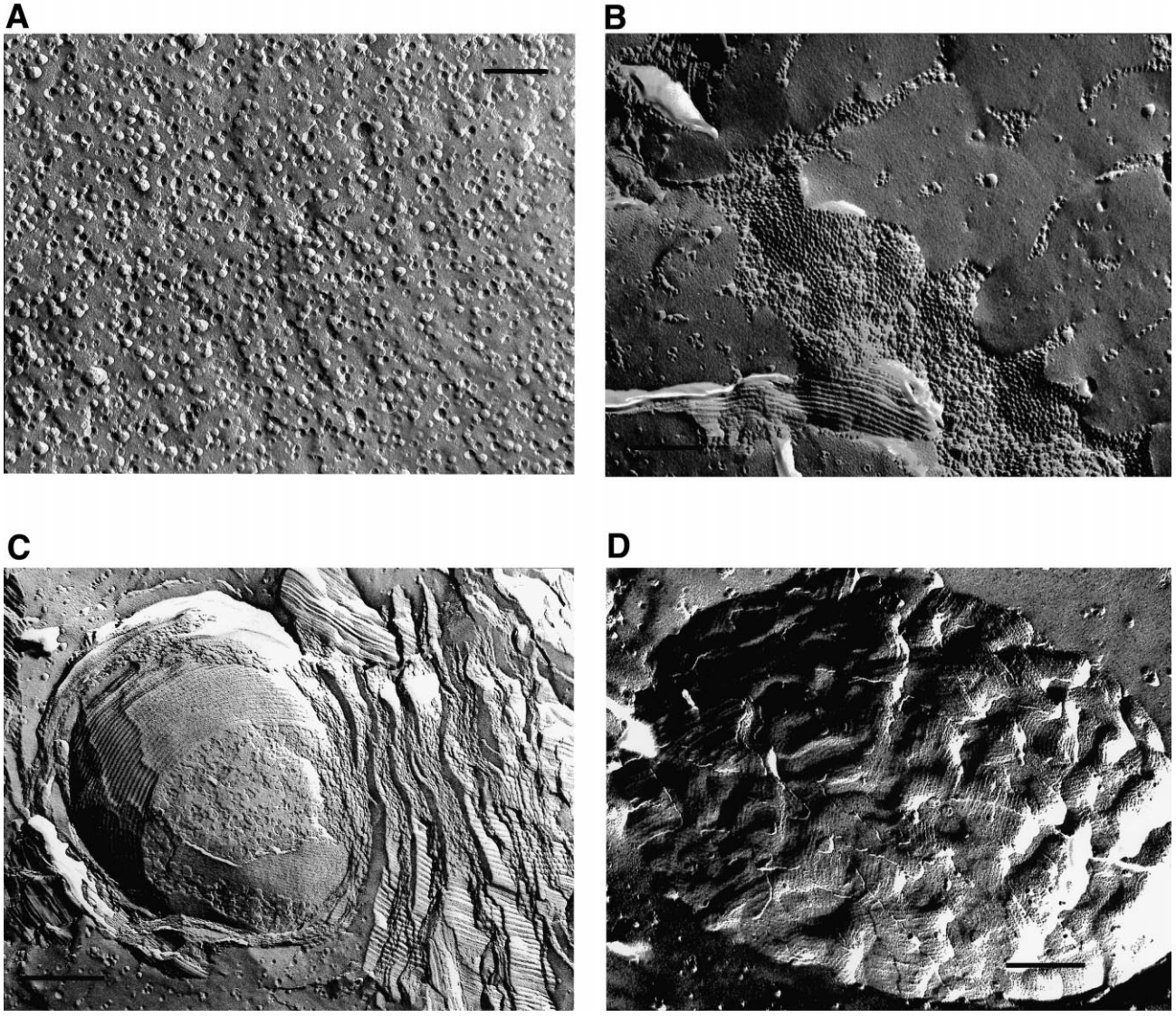

Fig. 2. Freeze-fracture electron microscopy of the coalescence process which occurs upon incubation of DMPC SUVs with rhIL-2. Time points were 0 h (A), 0.5 h (B,C), and 6 h (D). The reference bar equals 250 nm.

(see Section 2 for explanation) following 24 h incubation in the presence of rhIL-2, was 74% at 4°C, 94% at 19°C and 34% at 23°C. The optimal temperature thus appeared to be 19°C, a temperature between the pre- and main phase transitions of DMPC. The dependence of MLV formation on rhIL-2 was demonstrated by the minimal increase in turbidity for control SUVs in the absence of rhIL-2 over the same temperature range.

Creation of the multilamellar liposomes could have occurred as a result of either vesicle fusion or coalescence. Leakage experiments were performed to distinguish between these two possibilities. During vesicle fusion there is mixing of internal contents with minimal leakage [36–38]. In contrast, during vesicle coalescence leakage of internal contents occurs. DMPC SUVs were formed in the presence of 10 mM ANTS and 32 mM DPX. At these concentrations the DPX quenches the ANTS. The SUVs were washed by dialysis and incubated in the presence of rhIL-2 (DMPC:rhIL-2 at 250:1, by mass) at 19°C. Leakage of the water-soluble ANTS and DPX occurred during the process of forming multilayered vesicles resulting in reduced quenching of the ANTS

signal as both components were diluted by the surrounding buffer (Table 1). By 6 h about 12% of the internal contents had leaked compared to less than 2% for control SUVs incubated without rhIL-2. A 28% leakage was observed at 24 h. This observation, coupled with the freeze-fracture EM micrographs (Fig. 2) which showed large aggregates breaking up and annealing to form large MLVs, indicates that the process was primarily coalescence and not fusion.

Freeze-fracture electron microscopy was employed to follow the kinetics of the turbidity increase and to characterize the product. At various time points aliquots of the SUV/rhIL-2 sample incubated at 19°C were rapidly frozen between thin copper specimen carriers in preparation for freeze-fracture. The initial SUVs were ≤ 25 nm (Fig. 2A). At 30 min most of the replica revealed intact SUVs, but some regions revealed large aggregates or partially coalesced SUVs (Fig. 2B). Also seen at 30 min (Fig. 2C) were SUVs clearly flattening and coalescing to form bilayer sheets, as indicated by the characteristic $P_{\beta'}$ (ripple) phase typically observed for DMPC vesicles at this temperature. By 6 h (Fig. 2D) large multilayered vesicles were formed which contained bulges in the surface texture of the individual layers. Some SUVs were still present, indicating incomplete coalescence. By 24 h large multilayered vesicles were present with few uncoalesced SUVs (data not shown). The bulges were noted throughout the MLV structure, indicating that rhIL-2 was entrapped within the interlamellar spacings. The final liposomes had a mean diameter of 2.37 μm, as measured on an Accusizer 770 particle sizing system. The resultant multilayered vesicles were analyzed for the presence of rhIL-2, using the CTLL-2 bioassay. Activity was 2.17×10^6 IU/ml, with an 89% recovery and greater than 95% incorporation of rhIL-2 into vesicles.

The kinetics of the transition from SUVs to MLVs was also examined using DSC. As previously reported by Mabrey and Sturtevant [39], the starting DMPC SUVs exhibited a typical broad main phase transition at about 20°C followed by a small sharper transition at 25.7°C, the latter due to some multilayer contamination (Fig. 3, curve a). Upon incubation with rhIL-2, the broad transition peak appeared to break up into two separate peaks (Fig. 3, curve b). These in time vanished as the vesicles continued to coalesce (Fig. 3, curves c–e). The DSC tracing of the

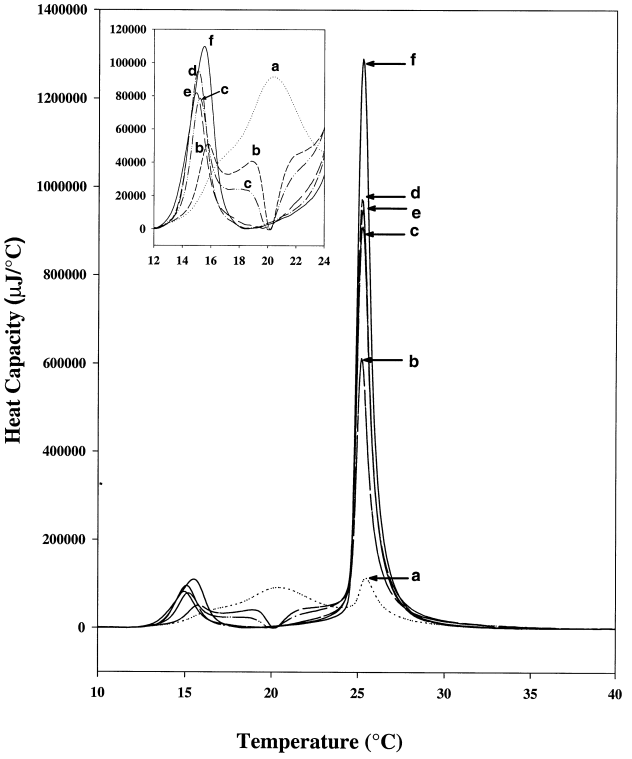

Fig. 3. DSC profile of rhIL-2-induced SUV coalescence. Scans were taken following an incubation at 19°C of DMPC SUVs and rhIL-2 at 200 mg/ml and 0.8 mg/ml respectively. Incubation times at 19°C were 0 min (a), 30 min (b), 2 h (c), 6 h (d), and 24 h (e). Control DMPC MLVs in the absence of rhIL-2 are also shown (f). Note that the actual measurements are not precisely at the time points stated, since approx. 20 min were required to lower the DSC cell temperature before beginning the heating scan at 20°C/h.

final product (Fig. 3, curve e) was identical to that of MLVs without rhIL-2 (Fig. 3, curve f), but with a 15% drop in the main phase transition enthalpy as well as a slight downward shift in the pretransition temperature.

The interactions of proteins or peptides with membranes are altered by pH and ionic strength, especially when they contain amphipathic helices [40,41] like the D α-helix of rhIL-2 [42]. To study the effect of pH on the coalescence process, turbidity was monitored at specific pH values at 19°C using citrate–phosphate buffer to adjust the pH of the reaction mixture. To minimize the effect on overall ionic strength (the reaction mixture contained 150 mM NaCl), the final citrate buffer concentrations were kept at 1–5 mM. As shown in Fig. 4A, coalescence of DMPC SUVs did not occur until the pH was

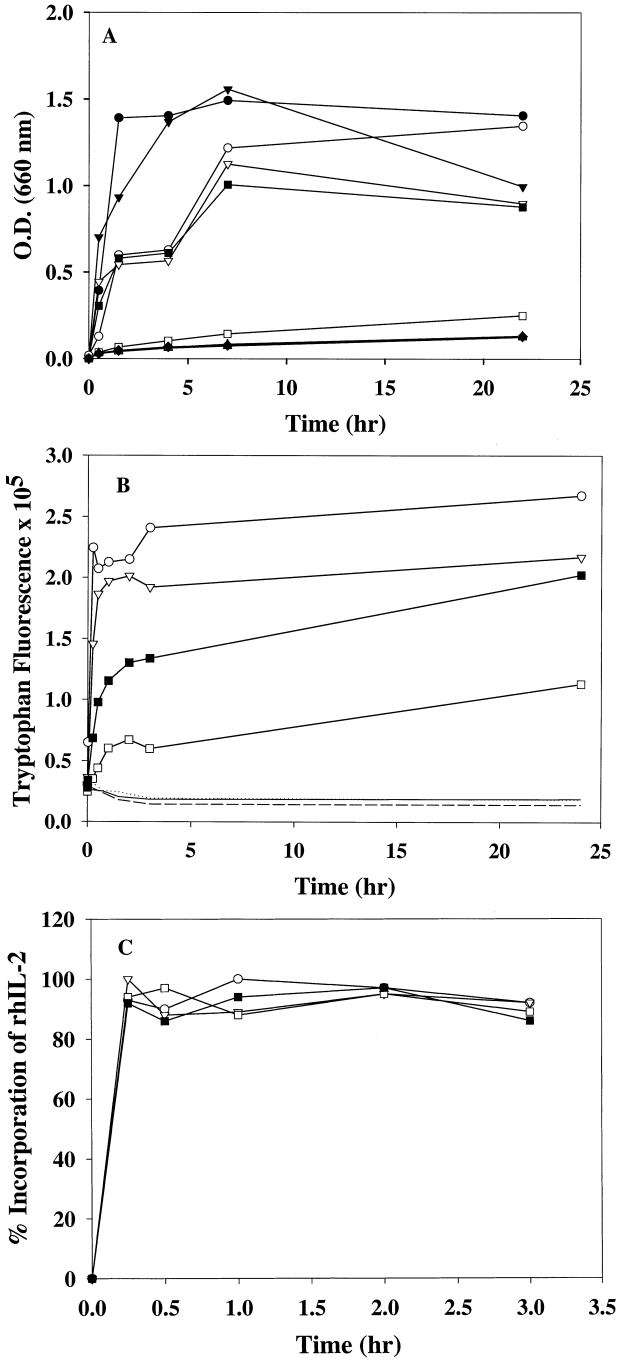

Fig. 4. The effect of pH on the kinetics of rhIL-2-induced DMPC SUV coalescence. The time course was measured at 19°C as a function of (A) turbidity, (B) tryptophan fluorescence, and (C) % incorporation of rhIL-2. The pH values employed were 3.6 (○), 4.0 (●), 4.5 (▼), 5.0 (▽), 5.5 (■), 5.9 (□), 6.6 (▲), 7.4 (△), and 8.2 (♦). The time course for rhIL-2 in the absence of DMPC SUVs is shown at pH 4 (solid line), pH 5 (dashed) and pH 6 (dotted).

below 6. Coalescence was abundant at and below pH 5.5, with an increase in both the rate and extent as the pH was lowered to 3.6. No significant coalescence was observed over this pH range in the absence of rhIL-2.

The effect of pH on rhIL-2-dependent coalescence of DMPC SUVs was further investigated by monitoring the fluorescence of the single tryptophan at position 121 in the native protein [43]. At pH 5.9 a slight increase in tryptophan fluorescence intensity was observed (Fig. 4B). As the pH of the reaction mixture was lowered, a time-dependent increase in tryptophan fluorescence intensity was observed. At low pH values the increase in fluorescence was rapid and leveled off by 6 h. Little further increase was

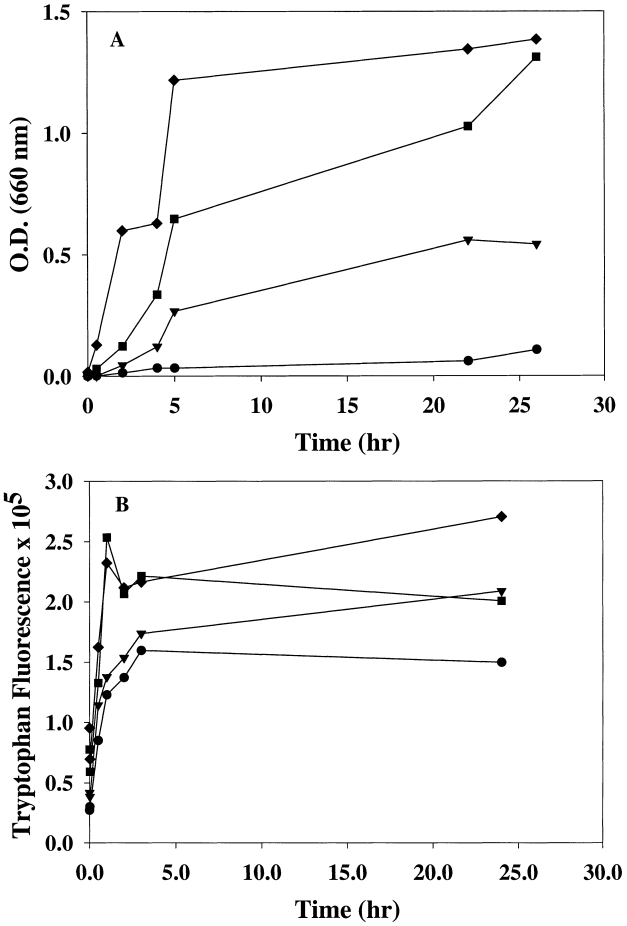

Fig. 5. The effect of ionic strength on the kinetics of rhIL-2-induced DMPC SUV coalescence. The time course was measured at 19°C as a function of (A) turbidity and (B) tryptophan fluorescence. The concentrations of NaCl employed were 0 mM (●), 10 mM (▼), 50 mM (■), and 150 mM (♦).

observed up to 24 h. The increase of tryptophan fluorescence in liposomal rhIL-2 over free rhIL-2 at the appropriate pH values was as much as 10-fold (Fig. 4B) and exhibited a 3–5 nm red shift in the tryptophan fluorescence maximum (data not shown).

The kinetics of the actual binding of rhIL-2 to SUVs at different pH values was monitored by removing an aliquot of the reaction mixture and measuring the rhIL-2 incorporation by the CTLL-2 bioassay. The binding appeared to be almost instantaneous, with greater than 90% of the rhIL-2 bound within 15 min for samples at pH 4.0, 5.0, 5.5 and 5.9 (Fig. 4C).

The effect of ionic strength on the rhIL-2-dependent coalescence process was examined using DMPC SUVs made in specified saline concentrations between 0 mM and 150 mM, all at pH 4 and 19°C (Fig. 5). Turbidity measurements (Fig. 5A) revealed an absence of coalescence at 0 mM NaCl and a steady increase as the salt concentration was raised to 150 mM. Tryptophan fluorescence measurements revealed a rapid initial increase in fluorescence intensity of about 5-fold at 0 and 10 mM NaCl and an almost 10-fold increase at 50 and 150 mM NaCl (Fig. 5B). Binding of rhIL-2, as determined by the CTLL-2 bioassay, was independent of saline concentration. Greater than 90% of the rhIL-2 was bound to the SUVs at all NaCl concentrations within the first 15 min of incubation (data not shown).

The data shown above demonstrated that the rhIL-2-dependent coalescence process was optimal at 19°C, at pH 4 and in 150 mM NaCl. During the formation of MLVs, lipid mixing must occur as the SUV bilayers merge to form the planar bilayers found in MLVs. Lipid mixing experiments (see Section 2 for details) were performed at 19°C in 150 mM NaCl and at pH 4 and 6. As expected from other experiments (Fig. 4), no lipid mixing was observed at pH 6 following 24 h (data not shown), while significant lipid mixing was found at pH 4. To examine the kinetics of the various stages in the coalescence process, Fig. 6 combines the pH 4 lipid mixing data with the early time point measurements of turbidity, tryptophan fluorescence and rhIL-2 incorporation (Fig. 4, pH 4 and 150 mM NaCl). The data are expressed as a percent of maximum values (6 h incubation time point). It is apparent that the rhIL-2 first bound to the SUVs (CTLL-2 results), followed by a structural change in the protein, as evidenced by the increase in tryptophan fluorescence. This in turn was followed by an increase in SUV aggregation, as indicated by a rise in turbidity, and then coalescence, as indicated by the lipid mixing data.

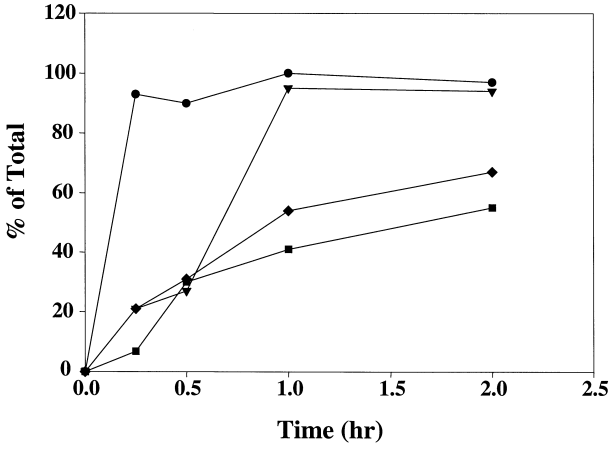

Fig. 6. The kinetics of the interaction of rhIL-2 with DMPC SUVs at pH 4, 150 mM NaCl. The % total refers to the % of the value after a 6 h incubation, the plateau of each of the effects monitored. The rhIL-2 binding as determined by the CTLL-2 bioassay (●), the increase in tryptophan fluorescence (▼), and the turbidity (◆) are from Fig. 4. Lipid mixing (■), an indication of coalescence, was determined by mixing DMPC SUVs with DMPC/NBD-PE/Rhod-PE (98.8:0.4:0.8, molar ratios) SUVs at a 19:1 ratio and incubating at 19°C with rhIL-2 at a lipid:protein mass ratio of 250:1.

Table 2
Coalescence of LUVs

Filter size (nm)	Initial (nm)	1 day (nm)	11 days (nm)
30	56	57 (29%) 1023 (71%)	2482
50	62	60	85
80	72	70	81
100	83	86	88
200	124	127	132

SUVs are known to be inherently more susceptible to fusogenic reagents than LUVs [44]. To test the size dependence of the coalescence process, DMPC LUVs of various sizes were made by extrusion through a series of polycarbonate filters. These LUVs were then incubated at 19°C with rhIL-2 at a lipid:protein mass ratio of 250:1 and a DMPC concentration of 200 mg/ml. As shown in Table 2, LUVs that were initially 56 nm in diameter yielded a mixture of coalescence products and unaltered vesicles following an

overnight incubation with rhIL-2. These LUVs continued to coalesce over a period of 11 days, yielding MLVs of approx. 2.5 μm in diameter. LUVs initially above 60 nm did not coalesce to any significant degree during the 11 day incubation period (Table 2), nor did any of the LUVs coalesce in the absence of rhIL-2. A more detailed examination of the rhIL-2 interaction with LUVs was performed on the 124 nm vesicles. The fluorescence of tryptophan did not change upon incubation overnight at 19°C at pH 6 (Fig. 7A). At pH 4, a 2-fold increase was observed by 5 h and a 5-fold increase at 24 h. Binding data based on the CTLL-2 bioassay again showed a rapid association of rhIL-2 at both pH values, although a maximum of only 80% incorporation was attained (Fig. 7B). An electron micrograph of the 124 nm vesicles

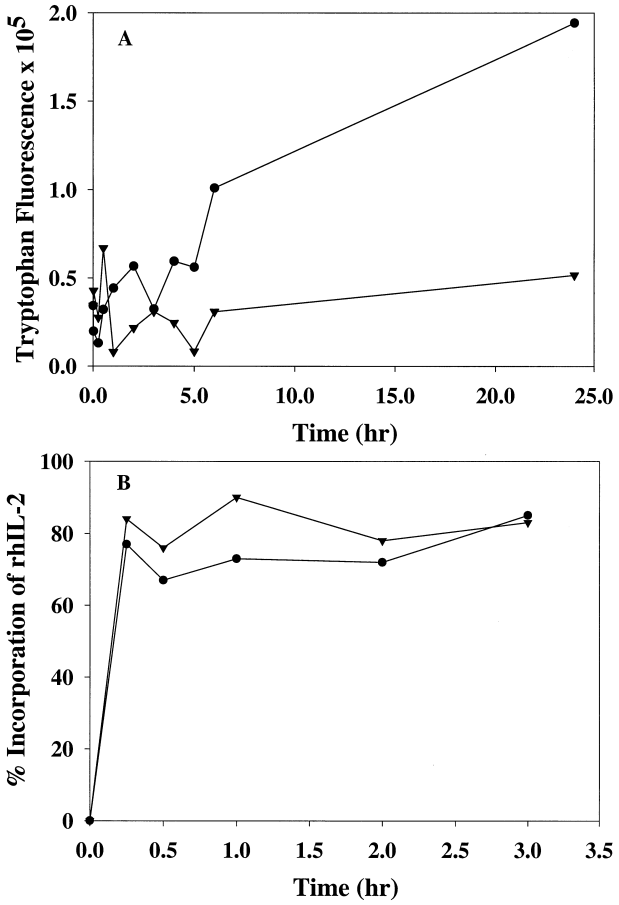

Fig. 7. The effect of pH on the kinetics of rhIL-2-induced DMPC LUV coalescence. The time course was measured as a function of (A) tryptophan fluorescence and (B) % incorporation of rhIL-2. The pH values employed were 4.0 (●) and 6.0 (▼).

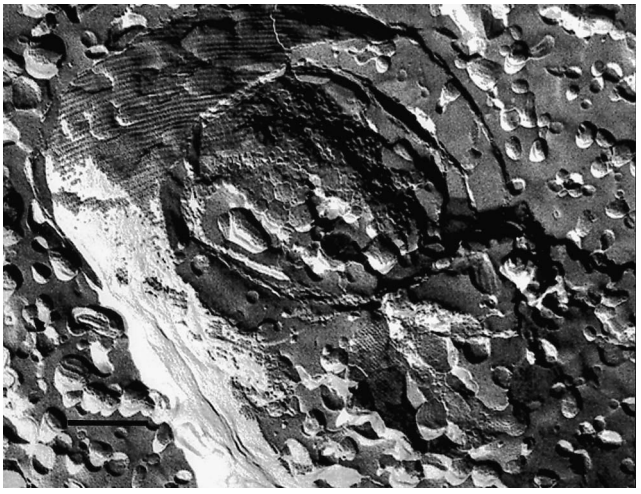

Fig. 8. Freeze-fracture electron microscopy of DMPC LUVs incubated with rhIL-2 for 24 h at 19°C. The initial LUVs were 124 nm. The reference bar equals 250 nm.

following a 24 h incubation at 19°C and pH 4 revealed many unaltered LUVs, consistent with the particle sizing data (Table 2). A few multilayered vesicles were present with incomplete or partially coalesced LUVs within the structures (Fig. 8).

4. Discussion

In this manuscript we describe a rhIL-2-dependent formation of MLVs from SUVs resulting in $>90\%$ incorporation of rhIL-2 into the multilamellar structures. Optimal conditions for the MLV formation were achieved when rhIL-2 was added to limit size ($\leq$25 nm) DMPC SUVs at 19°C (Fig. 1) in 150 mM NaCl at pH 4 (Figs. 4 and 5). The mechanism of MLV formation was determined to be coalescence, not fusion, based on leakage experiments (Table 1) and freeze-fracture EM (Fig. 2). The process was initiated by rapid binding of rhIL-2 to DMPC SUVs, which was then followed by a pH- and ionic strength-dependent conformational change in the protein (Figs. 4 and 6). Under optimal conditions, the latter step, as measured by the change in tryptophan fluorescence intensity, was complete by 1 h (Fig. 6). This appeared to promote SUV aggregation into large clusters. The large clusters formed intermediate structures (Figs. 2A–D and 3) which then annealed in time, resulting in the mixing of lipid

contents (Fig. 6) and formation of closed MLVs. These interpretations and a hypothetical mode of rhIL-2/bilayer interaction are discussed below.

The temperature at which the rhIL-2 interacted most favorably with DMPC SUVs was 19°C, based on the turbidity increase and coalescence efficiency. This is between the pretransition and main transition temperatures of DMPC MLVs, but within the main transition temperature of DMPC SUVs. The asymmetric distribution of phospholipid molecules in SUVs leads to the broader transition at a lower temperature and enthalpy than that of MLVs [39]. The enhanced ability of the rhIL-2 to interact with SUVs and induce coalescence at 19°C could be due to the looser, more distorted packing in the SUVs at this temperature. The diminished coalescence observed below the pretransition temperature (Fig. 1) could also be due in part to a competing spontaneous vesicle fusion event. Spontaneous fusion of SUVs composed of saturated lecithins to form vesicles of about 70 nm size is known to occur below the pretransition temperature of the phospholipid [45]. LUVs of this size range were found to resist rhIL-2-dependent coalescence to MLVs (Table 2).

Following the rapid association of rhIL-2 with DMPC SUVs, a conformational change in the protein was detected by an increase in tryptophan fluorescence intensity. rhIL-2 contains a single tryptophan located in the amphipathic D-helix. Polarized fluorescence decay of the tryptophan indicates that intramolecular quenching occurs in the native molecule [27]. A conformational change affecting the local environment of the tryptophan or its distance from a quenching moiety would result in an increase in fluorescence intensity. Just such an increase was observed following binding of rhIL-2 to SUV lipid bilayers (Fig. 4). The magnitude and kinetics of the change in tryptophan fluorescence intensity were dependent on both pH and ionic strength, being optimal at pH 4 and 150 mM NaCl (Figs. 4 and 5). A small red shift of 3–5 nm in the tryptophan emission wavelength maximum was also noted (data not shown). Such a shift would be consistent with hydrogen bonding or a dipole–dipole interaction involving the tryptophan imino group (vide infra). Changes in the tryptophan fluorescence intensity and emission maximum were not observed for free rhIL-2 over a wide pH range (Fig. 4B), demonstrating the dependence upon adsorption to the DMPC SUV bilayer. The conformational change involving Trp 121 of rhIL-2 appeared to precede the increased turbidity indicative of SUV aggregation and the subsequent lipid mixing and coalescence which resulted in MLV formation (Fig. 6).

Formation of MLVs proceeded through intermediate structures and was dependent upon vesicle coalescence. Aggregation of SUVs following rhIL-2 binding was detected by DSC and freeze-fracture EM. At both 30 min and 2 h a low enthalpy shoulder appeared prior to the main transition temperature observed for DMPC MLVs (Fig. 3, curves a, b). Additionally, a low enthalpy peak appeared above the pretransition temperature (Fig. 3, curve b). Both of these peaks appeared as the broad SUV main transition peak disappeared. The nature of these peaks could represent partially coalesced SUVs, as seen by freeze-fracture EM in Fig. 2B,C. Binding of rhIL-2 to DMPC SUVs (Fig. 2A) results in an aggregation of these vesicles (Fig. 2B). The large clusters coalesce through intermediate structures (Fig. 2C) to finally form the rhIL-2-rich MLV structures exhibiting their signature bulges and ripple phase (Fig. 2D).

Compared to control DMPC MLVs (without rhIL-2), the endotherms at both 6 and 24 h exhibited a 15% lower enthalpy for both the DMPC bilayer pre- and main phase transitions and did not show transition peak broadening. This is consistent with a surface or interfacial bound rhIL-2 removing a fraction of the lipid molecules from participating in the phase transitions [46].

In addition to its effect on the rhIL-2 conformational change (Fig. 5B), higher medium ionic strength likely influences the speed and extent of SUV coalescence (Fig. 5A) by reducing the Debye length of the Gouy–Chapman double layer surrounding the SUVs [47] and allowing a closer approach of DMPC bilayers. Coalescence would be enhanced by the proximity of opposing bilayers in conjunction with a local accumulation of a fusogenic molecule (rhIL-2) and bilayer defects (optimal approx. 19°C for DMPC). The increase in ionic strength may also participate in relieving the fluorescence quenching of tryptophan within SUV-bound rhIL-2 by neutralizing electrostatic interactions. Such neutralization could promote or stabilize the

conformational change(s) in rhIL-2, which may in turn promote the formation of bilayer defects.

Based on the above considerations, we propose a hypothetical mode of rhIL-2-induced SUV coalescence involving an interaction of tryptophan residue #121 of the amphipathic D α-helix of rhIL-2 with the bilayer interface of DMPC SUVs, leading to coalescence. In such an interaction, higher medium ionic strength would promote the proximity of opposing bilayers, while conformational change(s) in bound rhIL-2 would destabilize the DMPC SUV bilayers. The observed conformational change in rhIL-2 following binding to DMPC SUVs affects the tryptophan residue #121 environment, as demonstrated by the change in tryptophan fluorescence intensity. That this change in fluorescence could signal a direct role for tryptophan residue #121 at the bilayer interface is supported by studies of Yau et al. [48], who used ^{1}H magic angle spinning (MAS), two-dimensional nuclear Overhauser effect spectroscopy (2D-NOESY), ^{1}H MAS NMR and solid state ^{2}H NMR to study the interactions of tryptophan analogues with phosphatidylcholine membranes. They reported on the preference of tryptophan residues for membrane interfaces, specifically, in the vicinity of the glycerol group. This interaction caused modest changes in the acyl chain organization, with minimal penetration of tryptophan into the bilayer proper. These workers concluded that tryptophan's flat rigid shape limited its access to the hydrocarbon core. Moreover, its π electronic structure and associated quadrupolar moment (aromaticity) favored this electrostatically complex interface environment. The 3–5 nm red shift in the tryptophan fluorescence maximum noted above during the rhIL-2-dependent coalescence of SUVs would be consistent with the suggestion of Yau et al. [48] of an imino group hydrogen bonding or dipole–dipole interaction in this interfacial region. In addition, the DSC data (Fig. 3) and the freeze-fracture EM data (Fig. 2) exhibited an unperturbed $P_{\beta'}$ phase, which implies a minimal penetration of rhIL-2 into the DMPC bilayer's hydrocarbon core.

The lipid-bound rhIL-2 did not induce coalescence in the case of LUVs of >60 nm diameter (Table 2). Moreover, the increase in tryptophan fluorescence intensity was slower in the presence of LUVs than with SUVs and was only about 2-fold over the first 6 h (Fig. 7A). These observations are similar to those made with large multilamellar vesicles [27]. Since MLVs and LUVs possess relatively planar bilayer surfaces, a conformational change in rhIL-2 involving a partial penetration of tryptophan into the hydrocarbon core of the bilayer would be restricted. This could explain the longer time and only 2-fold increase in tryptophan fluorescence intensity. In addition, the already flat planar bilayers are not under the same strain as those of DMPC SUVs. Thus they would be less likely to fragment, a step required for the formation of multilamellar vesicles. The lack of LUV coalescence is consistent with previous studies demonstrating that LUVs are more stable than SUVs. SUVs, but not LUVs, exhibited lipid mixing at pH 5 in the presence of the peptide GALA [40] and LUVs were found to marginally fuse while SUVs displayed extensive fusion in the presence of PEG [44].

The coalescence phenomenon described in this paper is not limited to DMPC, as SUVs of other lipids including DPPC, DMPC/cholesterol, DMPC/DMPG and EPC exhibited varying degrees of coalescence in the presence of rhIL-2 (unpublished observations). Additionally, a similar ability to cause SUVs to coalesce has been noted for other cytokines of the hematopoietic family which possess α-helical bundle structures [49], such as granulocyte–macrophage colony stimulating factor (GM-CSF) and recombinant human Interleukin-4 (unpublished observations). Hence, the process offers a novel, scalable method for the manufacture of many different liposomal formulations composed of various cytokines of the hematopoietic family, forming MLVs with cytokine not just on the surface, but within the interlamellar spacings. This would allow for both a depot effect and altered pharmacological properties and biodistribution. Studies are underway to extend these observations to other cytokine families [49].

References

[1] J.F. Bazan, Science 257 (1992) 410–412.
[2] D.B. McKay, Science 257 (1992) 412–413.
[3] K.A. Smith, Science 240 (1988) 1169–1176.
[4] M.K. Jenkins, D.M. Pardoll, J. Mizuguchi, T.M. Chused, R.H. Schwartz, Proc. Natl. Acad. Sci. USA 34 (1987) 5409.

[5] M. Malkovsky, B. Loveland, M. North, G.L. Asherson, L. Gao, P. Ward, Nature 325 (1987) 262–265.
[6] E.A. Grimm, R.J. Robb, J.A. Roth, L.M. Neckers, L.B. Lachman, D.J. Wilson, S.A. Rosenberg, J. Exp. Med. 158 (1983) 1356–1361.
[7] J.B. Splawski, L.M. McAnally, P.E. Lipsky, J. Immunol. 144 (1990) 562–569.
[8] S.A. Rosenberg, J.J. Mule, P.J. Spiess, C.M. Reichert, S.L. Schwarz, J. Exp. Med. 161 (1985) 1169–1188.
[9] S.A. Rosenberg, M.T. Lotze, L.M. Muul, A.E. Chang, F.P. Avis, S. Leitman, W.M. Linehan, C.N. Robertson, R.E. Lee, J.T. Rubin, C.A. Seipp, C.G. Simpson, D.E. White, New Engl. J. Med. 316 (1987) 889–897.
[10] R. Whittington, D. Faulds, Drugs 46 (1993) 446–514.
[11] J.P. Siegal, R.K. Puri, J. Clin. Oncol. 9 (1991) 694–704.
[12] P.M. Anderson, E. Katsanis, A.S. Leonard, D. Schow, C.M. Loeffler, M.B. Goldstein, A.C. Ochoa, Cancer Res. 50 (1990) 1853–1856.
[13] E. Kedar, E. Braun, Y. Rutkowski, N. Emanuel, Y. Barenholz, J. Immunother. 16 (1994) 115–124.
[14] A. Adler, J. Schachter, Y. Barenholz, L.K. Bar, T. Klein, R. Korytnaya, A. Sulkes, R. Michowiz, Y. Cohen, I. Kedar, Cancer Biother. 10 (1995) 293–306.
[15] N. Gershman, D. Johnston, J.C. Bystryn, Vaccine Res. 3 (1994) 83–92.
[16] C.M. Loeffler, J.L. Platt, P.M. Anderson, E. Katsanis, J.B. Ochoa, W.J. Urba, D.L. Longo, A.S. Leonard, A.C. Ochoa, Cancer Res. 51 (1991) 2127–2132.
[17] S.F. Sencer, M.L. Rich, E. Katsanis, A.C. Ochoa, P.M. Anderson, Eur. Cytokine Netw. 2 (1991) 311–318.
[18] P.M. Anderson, D. Hasz, L. Dickrell, S. Sencer, Drug Dev. Res. 27 (1992) 15–31.
[19] J.J. Bergers, W. Den Otter, H.F.J. Dullens, C.T.M. Kerkvliet, D.J.A. Crommelin, Pharm. Res. 10 (1993) 1715–1721.
[20] F.J. Koppenhagen, Z. Küpcü, G. Wallner, D.J.A. Crommelin, E. Wagner, G. Storm, R. Kircheis, Clin. Cancer Res. 4 (1998) 1881–1886.
[21] O.C. Krup, I. Kroll, G. Böse, F.W. Falkenberg, J. Immunother. 22 (1999) 525–538.
[22] F.J. Koppenhagen, L.T.M. Balemans, P.A. Steerenberg, T.M. Jagmont, W. Den Otter, G. Storm, J. Liposome Res. 9 (1999) 313–329.
[23] P.M. Anderson, E. Katsanis, S.F. Sencer, D. Hasz, A.C. Ochoa, B. Bostrom, J. Immunother. 12 (1992) 19–31.
[24] M.E. Neville, K.W. Richau, L.T. Boni, L.E. Pflug, R.J. Robb, M.P. Popescu, Cytokine 12 (2000) 1702–1711.
[25] M.E. Neville, L.T. Boni, L.E. Pflug, M.C. Popescu, R.R. Robb, Cytokine 12 (2000) 1691–1701.
[26] W.C. Wimley, S.H. White, Nat. Struct. Biol. 3 (1996) 842–848.
[27] F.J. Koppenhagen, A.J.W.G. Visser, J.N. Herron, G. Storm, J.A. Crommelin, J. Pharm. Sci. 87 (1998) 707–714.
[28] G. Beschiaschvili, J. Seelig, Biochemistry 29 (1990) 52–58.
[29] R.M. Epand, L.T. Boni, S.W. Hui, Biochim. Biophys. Acta 692 (1982) 330–338.
[30] D.K. Struck, D. Hoekstra, R.E. Pagano, Am. Chem. Soc. 20 (1981) 4093–4099.
[31] B.N. Ames, Methods Enzymol. 8 (1966) 115–117.
[32] S. Gillis, M.M. Ferm, W. Ou, K.A. Smith, J. Immunol. 120 (1978) 2027–2032.
[33] A.J.H. Gearing, R. Thorpe, J. Immunol. Methods 114 (1988) 3–9.
[34] S.A. Ahmen, R.M. Gogal Jr., J.E. Walsh, J. Immunol. Methods 170 (1994) 211–224.
[35] J.P. Dufour, R. Nunnally, L. Buhle Jr., T.Y. Tsong, Biochemistry 20 (1981) 5576–5586.
[36] D. Gingell, L. Ginsberg, in: G. Poste, G.L. Nicolson (Eds.), Membrane Fusion, Elsevier/North-Holland Biomedical Press, New York, 1978, pp. 791–833.
[37] F. Szoka, in: A.E. Sowers (Ed.), Cell Fusion, Plenum Press, New York, 1987, pp. 209–240.
[38] S. Nir, J. Wilschut, J. Bentz, Biochim. Biophys. Acta 688 (1982) 275–278.
[39] S. Mabrey, J.M. Sturtevant, in: E.D. Korn (Ed.), Methods in Membrane Biology, Plenum Press, New York, 1978, pp. 237–274.
[40] R.A. Parente, S. Nir, F.C. Szoka Jr., J. Biol. Chem. 263 (1988) 4724–4730.
[41] J.F. Hunt, P. Rath, K.J. Rothschild, D.M. Engelman, Biochemistry 36 (1997) 15177–15192.
[42] R.M. Epand, R.F. Epand, R.C. Orlowski, R.J. Schlueter, L.T. Boni, S.W. Hui, Biochemistry 22 (1983) 5074–5084.
[43] T. Taniguchi, H. Matsui, T. Fujita, C. Takaoka, N. Kashima, R. Yoshimoto, J. Hamuro, Nature 302 (1983) 305–310.
[44] L.T. Boni, J.S. Hah, S.W. Hui, P. Mukherjee, J.T. Ho, C.Y. Jung, Biochim. Biophys. Acta 775 (1984) 409–418.
[45] C.F. Schmidt, D. Lichtenberg, T.E. Thompson, Biochemistry 20 (1981) 4792–4797.
[46] T.D. Bradrick, E. Friere, S. Georghiou, Biochim. Biophys. Acta 982 (1989) 94–102.
[47] N.O. Petersen, S.I. Chan, Biochim. Biophys. Acta 509 (1978) 111–128.
[48] W.M. Yau, W.C. Wimley, K. Gawrisch, S.H. White, Biochemistry 20 (1998) 14713–14718.
[49] N.A. Nicola (Ed.), Guidebook to Cytokines and Their Receptors, Oxford University Press, Oxford, 1994.